



# Effect of Fan on Inlet distortion: A Mixed fidelity Approach

Yunfei Ma, Jiahuan Cui, Nagabhushana Rao Vadlamani, Paul Tucker

► **To cite this version:**

Yunfei Ma, Jiahuan Cui, Nagabhushana Rao Vadlamani, Paul Tucker. Effect of Fan on Inlet distortion: A Mixed fidelity Approach. ISROMAC International Symposium on Transport Phenomena and Dynamics of Rotating Machinery, Dec 2017, Maui, United States. hal-02369305

**HAL Id: hal-02369305**

**<https://hal.archives-ouvertes.fr/hal-02369305>**

Submitted on 18 Nov 2019

**HAL** is a multi-disciplinary open access archive for the deposit and dissemination of scientific research documents, whether they are published or not. The documents may come from teaching and research institutions in France or abroad, or from public or private research centers.

L'archive ouverte pluridisciplinaire **HAL**, est destinée au dépôt et à la diffusion de documents scientifiques de niveau recherche, publiés ou non, émanant des établissements d'enseignement et de recherche français ou étrangers, des laboratoires publics ou privés.

# Effect of Fan on Inlet distortion: A Mixed fidelity Approach

Yunfei Ma<sup>1\*</sup>, Jiahuan Cui<sup>1</sup>, Nagabhushana Rao Vadlamani<sup>1</sup>, Paul Tucker<sup>1</sup>



ISROMAC 2017

International  
Symposium on  
Transport Phenomena  
and  
Dynamics of Rotating  
Machinery

Maui, Hawaii

December 16-21, 2017

## Abstract

Inlet distortion is typically encountered during the off-design conditions on civil aircrafts and in S-ducts in military aircrafts. It is known to severely deteriorate the performance of a gas-turbine engine. As the intakes get shorter, there is an increased interaction between the inlet distortion and the downstream fan. Previous studies in the literature use low-fidelity methods (RANS or URANS) to address this unsteady interaction, due the substantial computational cost associated with the high fidelity methods like LES/DNS. On the other hand, it is well known that the low order methods like RANS have limitations to accurately represent the distorted flows. In this paper, we propose a mixed-fidelity approach and employ it to study the intake-fan interaction at an affordable computational cost. The results demonstrate that there are two ways through which the fan affects the separated flow. Firstly, the suction effect of the fan alleviates the undesired distortion by ‘directly’ changing the streamline curvature, intensifying the turbulence transport and closing the recirculation bubble much earlier. Secondly, the enhanced turbulence in the vicinity of the fan feeds back into the initial growth of the shear layer by means of the recirculating flow. This ‘indirect’ feedback is found to increase the turbulence production during the initial stages of the shear layer. Both the direct and indirect effects of the fan significantly suppress the inlet distortion.

## Keywords

inlet distortion, fan effects, mixed fidelity

<sup>1</sup> *Department of Engineering, University of Cambridge, Cambridge, United Kingdom*

\*Corresponding author: ym324@cam.ac.uk

## INTRODUCTION

Flow distortion is typically encountered on the engine intakes and in the duct flows under the off-design conditions. The flow over an intake lip separates specifically during the take-off at high angles of incidence and under severe cross-winds during taxing or landing of an aircraft. The distorted flow at the inlet convects downstream and deteriorates the performance of the fan. In some extreme cases, it can even lead to the catastrophic events like stall and surge. Interestingly, as the inlets become shorter, the proximity of the fan to the source of the distortion is shown to affect the distortion recovery ([1]). In order to numerically investigate this interaction, it is crucial to accurately resolve the following flow regimes: (a) the separated flow domain and (b) the influence of a fan.

Most of the research in the literature addressed the fan-distortion study using low fidelity methods such as URANS and RANS [2, 3, 4]. It is well known that the predictive capability of these low fidelity approaches are satisfactory at the design point. However, they still suffer from severe limitations under off-design conditions, involving flow separation, distortion and unsteadiness [5, 6, 7]. In particular, when predicting flows with large-scale, low-frequency turbulence, the results may vary significantly among the different RANS models [5]. For these flows, eddy resolving simulations such as DNS/LES and hybrid LES/RANS are demonstrated to yield much more promising results [7, 8, 9].

On the other hand, the fan influence can be represented either by resolving all fan blades or with a body force. While

the former approach is computationally expensive [10], the Body Force Method (BFM) is much more economical[11] and practically feasible. BFM can be further classified into the smeared and standard methods, based on the extent to which the geometry has been modelled.

The Immersed Boundary Method with Smeared Geometry (IBMSG) is typically used to model the force field generated by a set of rotating blades. This approach assumes an infinite number of blades in the circumferential direction; which avoids the computational overhead of capturing the detailed blade geometry and/or incorporating moving boundaries to represent the fan. In this approach, an inviscid (or wall-normal) force and a viscous (or parallel) force due to the rotating blades are added to the circumferentially averaged Navier-Stokes equations. The inviscid component of the force, formulated by Marble [12], ensures that the flow follows the blade metal angle. The viscous component, introduced by Xu [13], accounts for the losses encountered over the blades using a force-velocity relation. Xu [13] has successfully employed this approach to investigate the distortion transfer in a high pressure turbine.

On the other hand, the standard Immersed Boundary Method (IBM) is generally used to resolve the features of a real geometry. Peskin [14] proposed IBM based on Eulerian and Lagrangian variables, linked by the interaction equations involving smooth approximation of the Dirac-delta function. This approach has been successfully applied by Fadlun [15] to study the flow past a backward facing step and by Defoe [16], who modelled a rotor blade and predicted the noise

propagation under the influence of an inlet flow distortion.

In this paper, a mixed-fidelity approach is applied to accurately investigate the influence of the fan on the inlet distortion at an affordable computational expense. The standard IBM proposed by Peskin [14] is used to model the distortion generator upstream of the fan. The unsteady separated regime downstream of the distortion generator is captured using a high-fidelity eddy resolving approach. Further downstream, IBMSG is used to model the force field due to a rotating fan. Subsequently, the recovery of distortion in the presence of a fan is examined using both the mean and turbulent characteristics.

## 1. NUMERICAL FRAMEWORK

Figure 1 illustrates the computational domain and the boundary conditions considered in the current study. This simplified setup is motivated by the experimental studies on the Darmstadt Rotor [17, 18, 19, 20, 21], albeit under different operating conditions. In these studies, the distortion generators were designed to reproduce the flow conditions in a real engine within the laboratory. Measurements by Lieser [17] and Bitter [20] show that the compressor performance is largely sensitive to the distortions encountered at the tip. Hence, a periodic distortion generator is placed upstream of the tip of the fan in order to reproduce the distortion encountered over the intake lip at high angles of attack. The test case employs the original duct and the rotating fan from the Bitter's test rig [20, 21], with the periodic beam installed upstream of the fan. It features a 30 deg sector duct with a distortion generator ('beam') of height ' $H$ ' and length ' $1.5H$ ' placed at an axial distance of ' $12.5H$ ' from the inlet. The fan is positioned at a streamwise distance of  $5.25H$  from the beam. All the spatial quantities mentioned in the following sections are normalised by the beam height  $H$ . The velocity is normalised by the velocity,  $u_\infty$ , measured at the maximum height of the beam (Fig.1), which corresponds to the outer edge velocity of a separated shear layer.

The primary objective of the current study is to capture the distortion generated on the lower wall. Hence, an inviscid boundary condition is imposed on the upper wall, which ensures that the pressure distribution due to the spinner is well represented at a reduced computational cost. International Standard Metric Conditions ( $P_0=101325\text{Pa}$  and  $T_0=288.15\text{K}$ ) are applied at the inflow and the massflow rate is fixed at  $10.6\text{kg/s}$ . This massflow rate corresponds to the peak efficiency point at 65% rotational speed ( $1361.31\text{rad/s}$ ). A radial equilibrium boundary condition is imposed at the outflow. Periodicity is imposed in the circumferential direction. The extent of the sector ( $30^\circ$  corresponds to  $5H$ ) is sufficient enough to ensure that the structures are decorrelated in the circumferential direction. In a mixed fidelity framework, the beam is represented using the conventional IBM [14]. The separated flow downstream of the beam is captured using the eddy resolving approach, while the force field of a rotating fan is replicated using IBMSG [22]). This approach avoids the need to capture detailed blade geometry or incorporate mov-

ing boundaries. Instead, it represents the force field generated by the rotating fan blades and captures the suction effect of the fan, thereby substantially reducing computational cost.

## 2. METHOD

The present simulations are carried out using a Rolls-Royce's in-house CFD code, HYDRA [23, 24]. Both IBM and IBMSG are implemented into the numerical framework and are thoroughly validated [1]. For the IBM part, the distortion generator is modelled using feedback forcing, proposed by Goldstein et al. [25]. It has the following expression,

$$f(\mathbf{x}, t) = \alpha \int_0^t \Delta \mathbf{u} dt + \beta \Delta \mathbf{u}, \quad (1)$$

$$\Delta \mathbf{u} = \mathbf{u}(\mathbf{x}_0, t) - \mathbf{u}_0(\mathbf{x}_0, t)$$

where the subscript 0 represents the solid boundary. The coefficients  $\alpha$  and  $\beta$  are negative constants because essentially they function as a proportional-integral (PI) feedback controller evaluated by the velocity difference. Eventually, the controller enforces  $\mathbf{u} = \mathbf{u}_0$  on the immersed boundary. From the viewpoint of control theory, the value of the force is independent of the two coefficients  $\alpha$  and  $\beta$ , under the condition that the computation is convergent. To ensure the convergence, the two coefficients should be carefully selected. In fact, they are associated with two important parameters: the frequency  $\frac{1}{2\pi} \sqrt{|\alpha|}$  and the damping factor  $-\frac{\beta}{2\sqrt{|\alpha|}}$ . Hence,

$\alpha$  must be large enough to keep the force frequency  $\frac{1}{2\pi} \sqrt{|\alpha|}$  much larger than any other frequencies in the flow [15]. This means that the feedback force should change rapidly and fit the flow to the desired direction within a unsteady period. Also, to ensure the numerical stability, the time step should also meet the requirement

$$\Delta t < \frac{-\beta - \sqrt{\beta^2 - 2\alpha k}}{\alpha}, \quad (2)$$

where the order of  $k$  is 1.

The fan modelled with IBMSG can be regarded as a set of an infinite number of infinitesimally thin blades. The forces are circumferential averaged into every cell in the blade region and turn the flow to the local desired direction. Cao et al. [22] introduced this method when studying intake separation and find this model is capable to capture the key flow features. Hence, we use this normal force model

$$f_n = -\frac{\mathbf{u}^l \cdot \mathbf{n}}{\Delta t} - \mathbf{RHS} \cdot \mathbf{n}, \quad (3)$$

where  $\mathbf{n}$  is the normal vector of blade surface, and  $\mathbf{RHS}$  is the right hand side of Navier-Stokes equation. The parallel force from Watson et al. [26] is also used, which is

$$f_p = -K(r)\rho u_{rel}^2, K(r) = 4k_1 s^2 + k_1, \quad (4)$$

where  $s$  is the fraction of span and the coefficient  $k_1$  need to be calibrated by the existing performance data. The blockage

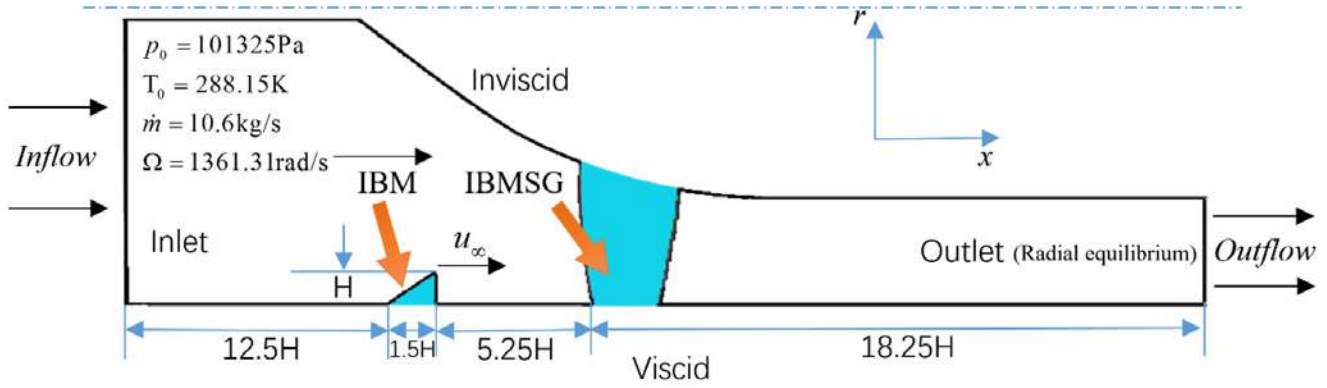


Figure 1. Experiment settings

effect is also modelled as [22],

$$\lambda = 1 - \frac{1}{2} \frac{(t_1 + t_2)}{S(r) \cos \beta}, \quad (5)$$

where  $t_1$  and  $t_2$  are the blade thickness for the pressure part and suction part, and  $S(r)$  is the surface pitch, as is shown in Figure 2.

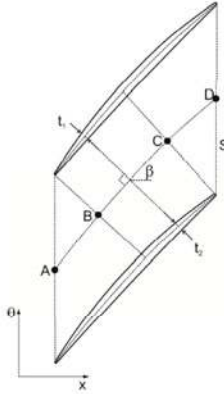


Figure 2. Sketch of blade blockage

### 3. RESULTS

#### 3.1 Instantaneous flow field

Figure 3 shows the contours of the stagnation pressure of the instantaneous flow. It demonstrates both the distortion generated in the lee of the beam and an increase in the stagnation pressure due the presence of the fan.

The iso-surfaces of  $Q$  ( $Q=40$ ) in different views are illustrated in Figure 4 and 5, contoured with the local axial velocity ( $v_x = -150 \sim 200$ ). The axial location of the fan is also shown by means of a sketch. Coherent two-dimensional detached shear layer forms at the edge of the beam which rapidly destabilized downstream. A decrease in the recirculation region is clearly evident in the presence of the fan. Qualitatively, an increase in the length scales of the turbulent structures due to fan is notable from the top-left subfigure in Fig. 5.

#### 3.2 Time averaged flow field

After flushing out the initial transience, statistics are collected for around  $94H/U_\infty$ . The maximal deviation of  $\langle u'u' \rangle$  extracted from two different times (with the interval of  $50H/U_\infty$ ) is only 5%, indicating the convergence is acceptable. Figure 6 compares the mean velocity profiles at different streamwise locations on a carpet plot. A line joining the locus of inflectional points of the velocity profiles is also overlaid. The recirculation region can be also seen in Figure 7. As noted from the instantaneous flow, the extent of the recirculation zone is significantly reduced due to the fan. The flow reattaches at an axial location which is more than a beam height upstream of the fan leading edge.

Figure 8a shows the contours of the time-averaged turbulent kinetic energy. The TKE in the shear layer and in the reattaching regime has increased by around 40-70% in the axial direction in the presence of fan. This is partially caused by a higher production in the shear layer (Fig. 8b) and partially by a stronger convection in the middle-rear part of the recirculation region (Fig. 8c).

#### 3.3 Mechanism

To further investigate how fan interacts the separation bubble through turbulence, this section delves into the mechanism by which the fan has reduced the recirculation region. In the previous section, Figure 8b and 8c demonstrates a substantial increase in both the production and convection. However, the location of such increase varies, and consequently may present different traits. To examine this in more details, the individual contributions from the dominant terms (in order):  $\langle u'u' \rangle \partial U / \partial x$ ,  $\langle v'v' \rangle \partial V / \partial y$  and  $\langle u'v' \rangle \partial U / \partial y$  to the TKE production are analysed.

The results demonstrate that there are two distinct ways through which the fan effects the separated flow: shear flow dominant (Zone 1) and strain rate dominant (Zone 2), shown in Figures 9a and 9b. In Zone 2, the primary effect of the fan is observable between  $x = 2H - 4H$  where the recirculation region decreases due to the change of the streamline curvature. Both  $\langle u'u' \rangle$  and  $\langle v'v' \rangle$  increase significantly within this region by around 40% and 75% respectively. The increase in  $\langle v'v' \rangle$  is much more pronounced than  $\langle u'u' \rangle$ , in-

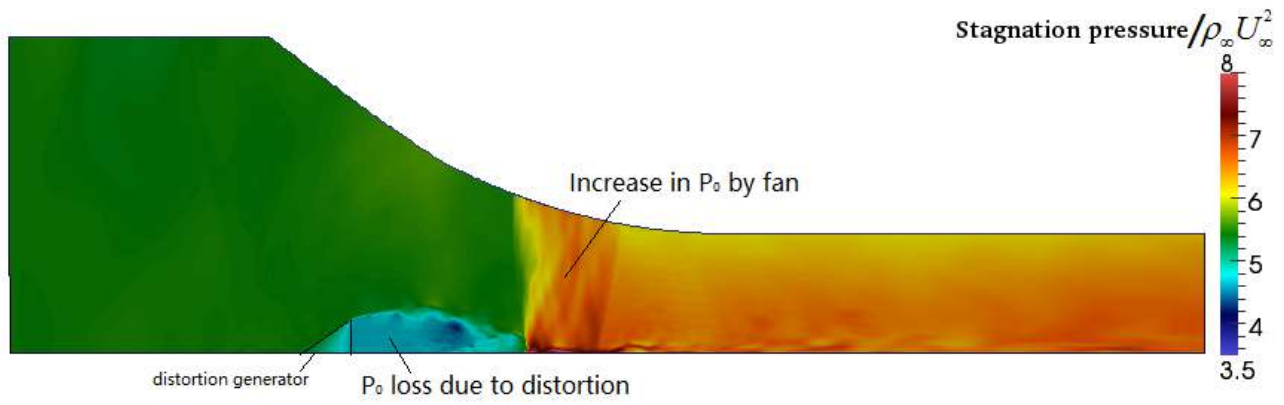


Figure 3. Total pressure distribution

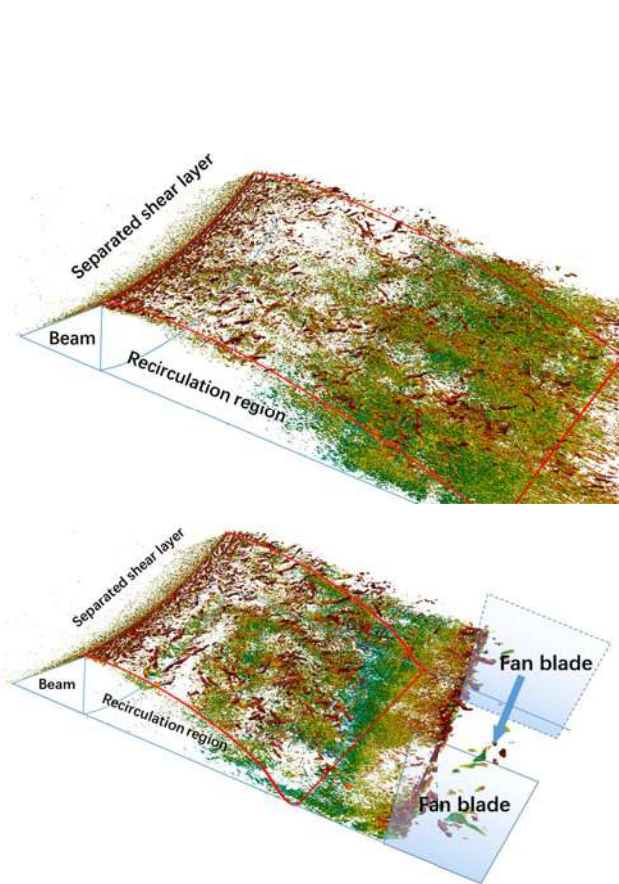


Figure 4. Instantaneous flow for the cases without/with fan

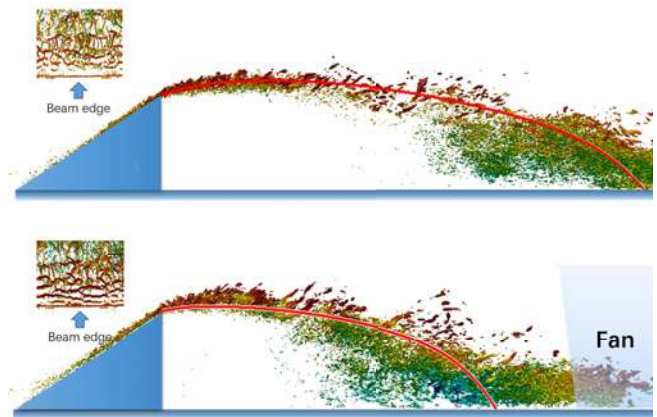


Figure 5. Lateral view of instantaneous flow for the cases without/with fan

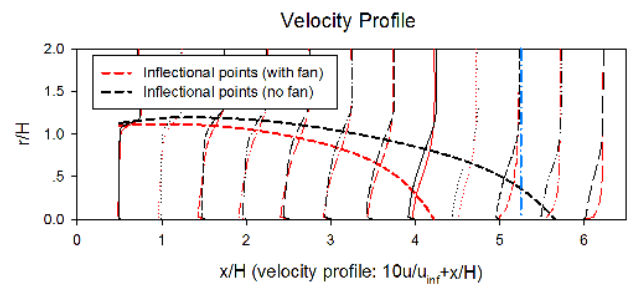


Figure 6. Velocity profile

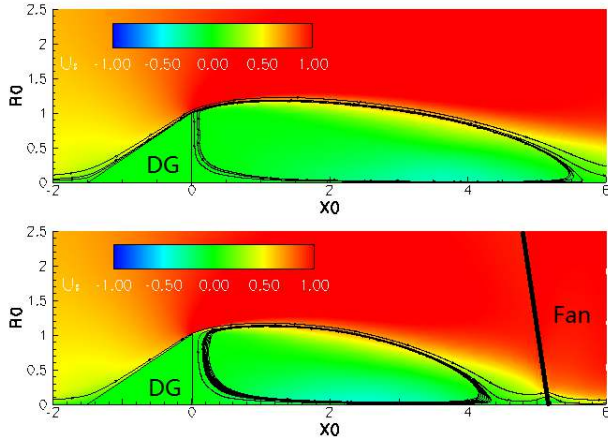


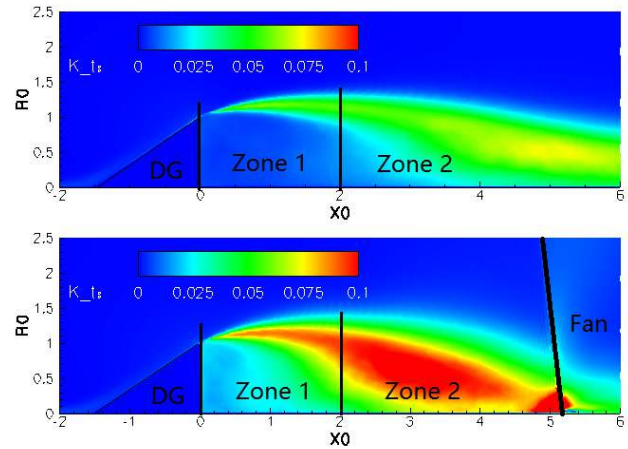
Figure 7. Recirculation region

dicating a stronger turbulent transport in the wall-normal direction. This is similar to that observed in the context of corner separation [27] separating at the leading edge of the blade. Consistent with the observations of Bradshaw [28], we consider this increase in Reynolds stresses to be a ‘direct effect’ which is attributed to the additional strain rate caused by the curvature change.

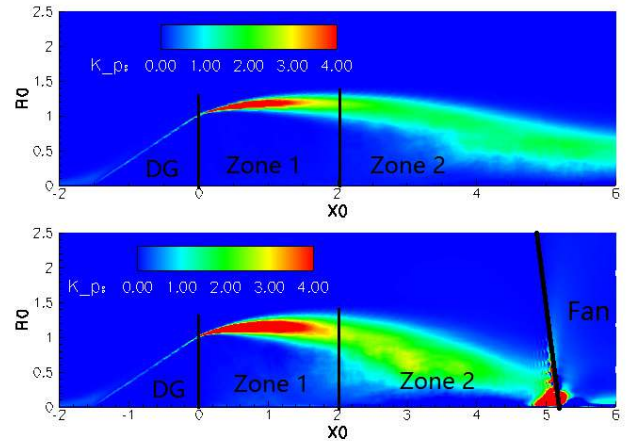
In zone 1, Figures 9a and 9b also demonstrate an increase in both the streamwise and wall normal fluctuations within the shear layer at the edge of the beam between  $x = 0 - 2H$ . Clearly, the spreading rate of the shear layer is much more predominant in the presence of the fan. This is attributed to the ‘indirect effect’ of the fan, where the enhanced turbulence generated in the vicinity of the fan feeds back into the origin of the shear layer by means of the recirculating flow. This is also evident from the Figures 8a and 8c where an increase in the TKE and TKE convection is observable within the recirculating region. Consequently, this ‘indirect’ feedback is found to further intensify the turbulence production within the shear layer (Figure 8b) increasing the Reynolds stresses ( $\langle u'u' \rangle$ ,  $\langle v'v' \rangle$ ).

As expected,  $\langle u'v' \rangle \partial U / \partial y$  is found to be the major contributor to the total production of TKE in Zone 1 within a spreading shear layer. Figure 10 compares the velocity gradients  $\partial U / \partial y$  to the contours of the Reynolds stress  $\langle u'v' \rangle$  (Fig.9c) without/with fan. It is evident that the contribution to the TKE production is primarily affected by an increase in the Reynolds stress  $\langle u'v' \rangle$ . On the other hand, the change in the velocity gradients is marginal.

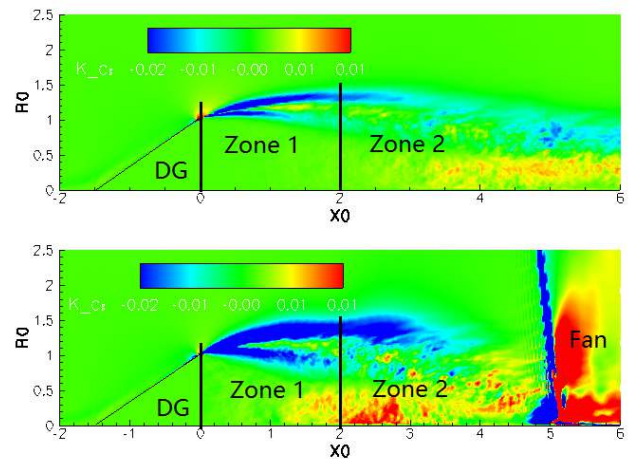
The increased TKE in Zone 1 is subsequently convected downstream into the Zone 2 through the mainstream flow and resulting in the cyclic feedback between both the zones. Hence, although the flow in the Zone 1 is not affected directly by the fan, it is still a key source of turbulence due to the feedback from the reverse flow. It supplements the turbulence generated in the vicinity of the fan in the Zone 2 and also contributes to the earlier reattachment of the separation bubble.



(a) Contours of TKE

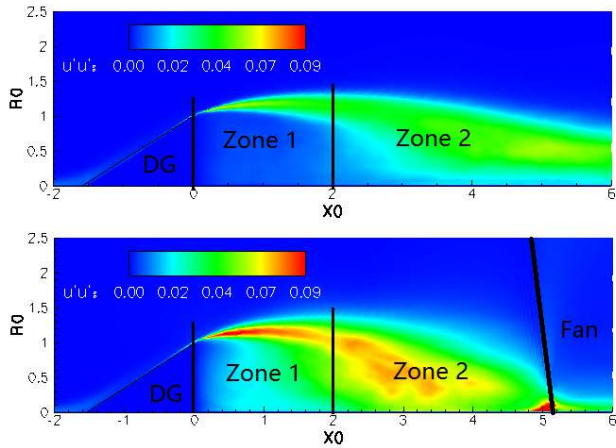


(b) Contours of TKE Production

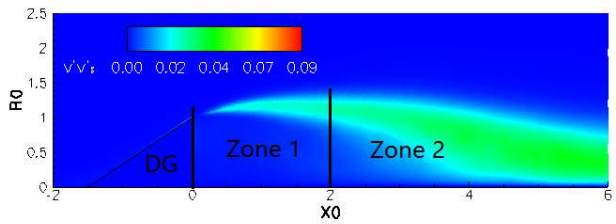


(c) Contours of TKE convection

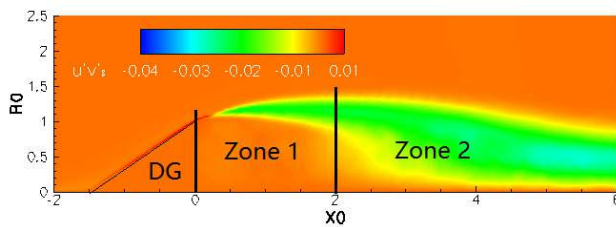
Figure 8. Turbulent Kinetic Energy Statistics



(a) Reynolds stress  $\langle u'u' \rangle$



(b) Reynolds stress  $\langle v'v' \rangle$



(c) Reynolds stress  $\langle u'v' \rangle$

Figure 9. Main Reynolds stresses

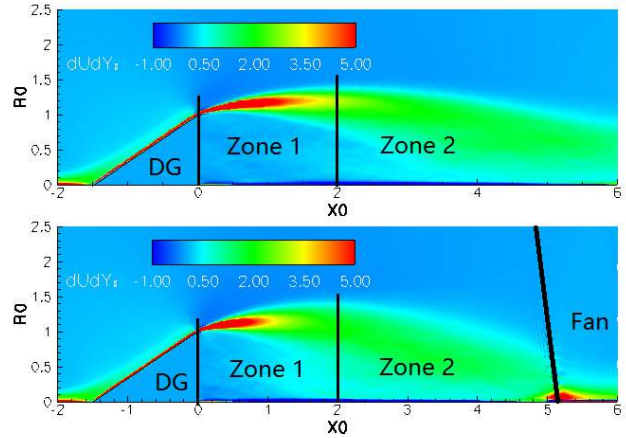


Figure 10. Velocity gradient  $\partial U / \partial y$

#### 4. CONCLUSION

In this paper, we propose a mixed-fidelity approach and employ it to study the intake-fan interaction at an affordable computational cost. The results demonstrate that there are two ways through which the fan effects the separated flow: Firstly, the suction effect of the fan (effective upto almost half the chord length upstream of the fan) alleviates the undesired distortion by ‘directly’ changing the streamline curvature, intensifying the strain rate and turbulence transport thereby closing the recirculation bubble much earlier. Secondly, the enhanced turbulence in the vicinity of the fan feeds back into the initial growth of the shear layer by means of the recirculating flow. This ‘indirect’ feedback is found to increase the turbulence production and spreading rate of the shear layer. Both these direct and indirect effects of the fan significantly suppress the inlet distortion.

From an engineering perspective, the current study shows that the loading of the fan blade can be conveniently altered to maximise the stagnation pressure recovery by suppressing the distortion. A tip loaded fan can increase the streamline curvature driving early reattachment of the flow. Further studies will be carried out to address these aspects and explore the possibility of some potential flow control methods to alleviate the inlet distortion.

#### ACKNOWLEDGMENTS

The authors gratefully acknowledge the UK Turbulence Consortium grant (EPSRC grant EP/L000261/1), the financial support from the Chinese Scholarship Council, and the technical support from Rolls-Royce.

#### REFERENCES

- [1] Teng Cao, Nagabhushana Rao Vadlamani, Paul G Tucker, Angus R Smith, Michal Slaby, and Christopher TJ Sheaf. Fan–intake interaction under high incidence. *Journal of Engineering for Gas Turbines and Power*, 139(4):041204, 2017.

- [2] V Jerez Fidalgo, CA Hall, and Y Colin. A study of fan-distortion interaction within the nasa rotor 67 transonic stage. *Journal of Turbomachinery*, 134(5):051011, 2012.
- [3] Sebastian Barthmes, Jakob P Haug, Andreas Lesser, and Reinhard Niehuis. Unsteady cfd simulation of transonic axial compressor stages with distorted inflow. In *Advances in Simulation of Wing and Nacelle Stall*, pages 303–321. Springer, 2016.
- [4] John Seddon and Eustace Laurence Goldsmith. *Intake aerodynamics*. Amer Inst of Aeronautics &, 1999.
- [5] Paul Tucker and Yan Liu. Turbulence modeling for flows around convex features. In *44th AIAA Aerospace Sciences Meeting and Exhibit*, page 716, 2006.
- [6] Nicolas Gourdain, Laurent YM Gicquel, and Elena Colado. Comparison of rans and les for prediction of wall heat transfer in a highly loaded turbine guide vane. *Journal of propulsion and power*, 28(2):423–433, 2012.
- [7] Yangwei Liu, Hao Yan, Lipeng Lu, and Qiushi Li. Investigation of vortical structures and turbulence characteristics in corner separation in a linear compressor cascade using ddes. *Journal of Fluids Engineering*, 139(2):021107, 2017.
- [8] PR Spalart and DR Bogue. The role of cfd in aerodynamics, off-design. *The Aeronautical Journal (1968)*, 107(1072):323–329, 2003.
- [9] Feng Gao, Wei Ma, Jinjing Sun, Jérôme Boudet, Xavier Ottavy, Yangwei Liu, Lipeng Lu, and Liang Shao. Parameter study on numerical simulation of corner separation in lmfa-naca65 linear compressor cascade. *Chinese Journal of Aeronautics*, 30(1):15–30, 2017.
- [10] Jeffrey Slotnick, Abdollah Khodadoust, Juan Alonso, David Darmofal, William Gropp, Elizabeth Lurie, and Dimitri Mavriplis. Cfd vision 2030 study: a path to revolutionary computational aerospace. 2014.
- [11] Roberto Verzicco, Jamaludin Mohd-Yusof, Paolo Orlandi, and Daniel Haworth. Large eddy simulation in complex geometric configurations using boundary body forces. *AIAA journal*, 38(3):427–433, 2000.
- [12] FRANK E Marble. Three-dimensional flow in turbomachines. *High Speed Aerodynamics and Jet Propulsion*, 10:83–166, 1964.
- [13] L Xu. Assessing viscous body forces for unsteady calculations. In *ASME Turbo Expo 2002: Power for Land, Sea, and Air*, pages 323–331. American Society of Mechanical Engineers, 2002.
- [14] Charles S Peskin. The immersed boundary method. *Acta numerica*, 11:479–517, 2002.
- [15] EA Fadlun, R Verzicco, Paolo Orlandi, and J Mohd-Yusof. Combined immersed-boundary finite-difference methods for three-dimensional complex flow simulations. *Journal of computational physics*, 161(1):35–60, 2000.
- [16] Jeffrey J Defoe and Zoltán S Spakovszky. Effects of boundary-layer ingestion on the aero-acoustics of transonic fan rotors. *Journal of Turbomachinery*, 135(5):051013, 2013.
- [17] JA Lieser, C Biela, CT Pixberg, H-P Schiffer, S Schulze, A Lesser, CJ Kähler, and Niehuis R. Compressor rig test with distorted inflow using distortion generators. 2011.
- [18] R Niehuis, A Lesser, Axel Probst, Rolf Radespiel, Sonja Schulze, Christian Kähler, Frank Spiering, and Norbert Kroll. Simulation of nacelle stall and engine response. 2013.
- [19] Simon Übelacker, Rainer Hain, and Christian J Kähler. Flow investigations in a stalling nacelle inlet under disturbed inflow. In *Advances in Simulation of Wing and Nacelle Stall*, pages 271–283. Springer, 2016.
- [20] Martin Bitter, Fabian Wartzek, Simon Übelacker, Heinz-Peter Kähler Schiffer, and Christian J. Characterization of a distorted transonic compressor flow using dual-luminophore pressure-sensitive paint. In *10th Pacific Symposium on Flow Visualization and Image Processing (PSFVIP-10), fedOA (Federico II Open Archive), Naples, Italy*, 2015.
- [21] Fabian Wartzek, Felix Holzinger, Christoph Brandstetter, and Heinz-Peter Schiffer. Realistic inlet distortion patterns interacting with a transonic compressor stage. In *Advances in Simulation of Wing and Nacelle Stall*, pages 285–302. Springer, 2016.
- [22] Teng Cao, Paul Hield, and Paul G Tucker. Hierarchical immersed boundary method with smeared geometry. In *54th AIAA Aerospace Sciences Meeting*, page 2130, 2016.
- [23] PI Crumpton, P Moinier, and MB Giles. An unstructured algorithm for high reynolds number flows on highly stretched grids. *Numerical methods in laminar and turbulent flow*, pages 561–572, 1997.
- [24] L Lapworth. Hydra-cfd: a framework for collaborative cfd development. In *International Conference on Scientific and Engineering Computation (IC-SEC), Singapore, June*, volume 30, 2004.
- [25] D Goldstein, R Handler, and L Sirovich. Modeling a no-slip flow boundary with an external force field. *Journal of Computational Physics*, 105(2):354–366, 1993.
- [26] Rob Watson, Jiahuan Cui, Yunfei Ma, and Paul Hield. Improved hierarchical modelling for aerodynamically coupled systems. In *ASME Turbo Expo 2017: Turbine Technical Conference and Exposition*. American Society of Mechanical Engineers, 2017.
- [27] Yangwei Liu, Hao Yan, Yingjie Liu, Lipeng Lu, and Qiushi Li. Numerical study of corner separation in a linear compressor cascade using various turbulence models. *Chinese Journal of Aeronautics*, 29(3):639–652, 2016.
- [28] Peter Bradshaw. Effects of streamline curvature on turbulent flow. Technical report, DTIC Document, 1973.